

The Cool ISM in Elliptical Galaxies. II. Gas Content in the Volume - Limited Sample and Results from the Combined Elliptical and Lenticular Surveys

Gary A. Welch

Saint Mary's University

Department of Astronomy and Physics

Halifax, Nova Scotia B3H 3C3

Canada

`gwelch@ap.smu.ca`

and

Leslie J. Sage

University of Maryland

Department of Astronomy

College Park, Maryland 20742

USA

`lsage@astro.umd.edu`

and

Lisa M. Young

New Mexico Institute of Mining and Technology

Department of Physics

Socorro, New Mexico, and

Adjunct Astronomer at the National Radio Astronomy Observatory

`lyoung@physics.nmt.edu`

ABSTRACT

We report new observations of atomic and molecular gas in a volume limited sample of elliptical galaxies. Combining the elliptical sample with an earlier and similar lenticular one, we show that cool gas detection rates are very similar among low luminosity E and SO galaxies but are much higher among luminous SOs. Using the combined sample we revisit the correlation between cool gas mass and blue luminosity which emerged from our lenticular survey, finding strong support for previous claims that the molecular gas in ellipticals and lenticulars has different origins. Unexpectedly, however, and contrary to earlier claims, the same is *not true* for atomic gas. We speculate that both the AGN feedback and merger paradigms might offer explanations for differences in detection rates, and might also point towards an understanding of why the two gas phases could follow different evolutionary paths in Es and SOs. Finally we present a new and puzzling discovery concerning the global mix of atomic and molecular gas in early type galaxies. Atomic gas comprises a greater fraction of the cool ISM in more gas rich galaxies, a trend which can be plausibly explained. The puzzle is that galaxies tend to cluster around molecular-to-atomic gas mass ratios near either 0.05 or 0.5.

Subject headings: galaxies: elliptical and lenticular, cD - galaxies: evolution - galaxies: ISM

1. INTRODUCTION

With this paper we conclude our surveys of atomic and molecular gas in volume limited samples of elliptical and lenticular galaxies (SOs: Welch & Sage (2003), Sage & Welch (2006); Es: Sage et al. (2007), Paper I). The prime motivation for our work has been to address the long-standing mystery of why those kinds of galaxies typically have much less cool gas than their stars have returned over the last 10 Gyr. We have accepted the penalty of long integration times in order to finesse possibly serious biases in earlier studies - towards optically luminous galaxies and/or those already known or suspected to contain large amounts of gas - and also in order to probe for cool gas at mass limits far below those implied by our current understanding of stellar evolution.

2. OBSERVATIONS AND DATA REDUCTION

2.1. Data from the GBT and IRAM 30m Telescopes

The properties of the sample have been described in Paper I. The 22 HI spectra presented here were recorded at the NRAO Robert C. Byrd Green Bank Telescope (GBT)¹ in April 2007. At the frequency of the 21cm hyperfine transition the GBT has FWHM=8.7'. Sensitivity limits were designed to provide 5σ detections, or upper limits, of $0.02M_e$, where M_e is the mass of gas returned within a 10 Gyr old galaxy according to Faber & Gallagher (1976). Observations were conducted in seven 2-9 hour sessions between 21 and 28 April. Each session included flux calibration on either 3C 48 or 3C 286 and a scan of a spiral galaxy with strong HI emission. Calibration observations were omitted during two sessions which immediately followed another program using the same backend setup. The observing unit was a standard on-off sequence in which 150 seconds each were spent on the source and nearby sky. Off positions were located either one-half degree east or west of the galaxy to avoid spurious emission from objects known from the NASA Extragalactic Database to be at a similar redshift. Data was reduced with GBTIDL following standard procedures. Occasional bad scans were deleted and noise spikes removed. The baseline on each summed, smoothed spectrum was defined by a window from 2000 to 4000 km s⁻¹ wide, except 1000 km s⁻¹ wide in the case of UGCA 298. The baseline window was centered on the galaxy optical velocity whenever possible, but was shifted to avoid Galactic foreground emission for low redshift objects. The line window (Column 2 in Table 1) was chosen to include visible emission, otherwise it was centered on the systemic velocity and its width set equal to twice the measured stellar velocity dispersion. First- or second-order polynomial fits were generally found to be satisfactory, although 4th order fits were made in the case of NGC 584, 636, 1172 and 4125. Spectra were binned to 5.12 km s⁻¹ resolution.

In June 2007 the IRAM 30m telescope on Pico Veleta, Spain was used to search 24 galaxies for CO emission in the J=1-0 and J=2-1 transitions. The telescope has FWHM=21'' and 11'', respectively, at the frequencies of those transitions. Single pointed observations were made in all cases. Sensitivity requirements on the J=(1-0) transition were derived using the same criterion as for the GBT sessions, and observing procedure followed the same pattern as in previous visits to the 30m telescope (Welch & Sage 2003). CLASS was used for data reduction, and standard procedures explained in our earlier papers were followed. A linear baseline was subtracted from each summed scan, and line windows were defined in the same way as for the HI data. Final spectra were binned to resolutions of 10.4 km s⁻¹, except 13

¹The National Radio Astronomy Observatory is a facility of the National Science Foundation operated under cooperative agreement by Associated Universities Inc.

km s⁻¹ in the case of the CO(1-0) spectra of NGC 821 and NGC 4308.

Figure 1 shows the final, baseline-subtracted spectra. We have included a few CO spectra from Paper I in order to facilitate comparison with the new HI observations. A summary of the measurements made from the new data is presented in Table 1.

2.2. The Impact of Differing Telescope Beam Sizes

The beam sizes of the HI and CO observations are very different (9' and 21'' for HI and CO(J=1-0), respectively). Naturally, then, these data are not appropriate for comparisons of local HI and H₂ surface densities. We believe, however, that they can be used to determine total gas masses with accuracies sufficient for the purposes of this investigation. HI emission in local elliptical and lenticular galaxies has been mapped with the VLA and WSRT by Sage & Welch (2006), Morganti et al. (2006), and Oosterloo et al. (2007). HI maps of 4 low luminosity ellipticals have been published by Lake et al. (1987). The detected gas is usually several arcminutes (several tens of kpc) in diameter. In the case of very gas rich systems or systems with close companion galaxies (our selection criteria generally exclude the latter) the atomic gas extends up to 10' in diameter. Inspecting maps published in the above works indicates that the GBT (median beam diameter ~50 kpc for our E and S0 galaxies) would see most of the emission in most cases, especially in low luminosity galaxies, although quantifying that impression is difficult. The Arecibo telescope (median beam diameter ~15 kpc for our samples) has been used by ourselves (Sage & Welch 2006) to measure M(HI) in 6 galaxies, and by several previous workers whose results we have included. It is possible that Arecibo has missed appreciable emission in a few galaxies, but we lack interferometer observations to quantify the situation.

Turning to the molecular phase, the regions sampled by the 30m telescope have median diameters of 1.8 and 1.7 kpc for E and S0 galaxies, respectively. As part of our lenticular survey (Welch & Sage 2003) unpublished CO observations at several positions across five galaxies (NGC3607, NGC4150, NGC4310, NGC4460, NGC5866) were made with the 30m Telescope. It was found that the central pointing accounts for about half (median value 57%) of the total emission seen at all positions. That result is consistent with comparisons by one of us (Young) of 30m fluxes with interferometer maps (Young 2002, 2005; Young et al. 2008) of CO emission in a number of E and S0 galaxies. Consequently we believe that the values of M(H₂) presented in the present work can be taken to represent the total molecular gas mass to within a factor of $\lesssim 2$.

Thus, even though the beam sizes for HI and CO are quite different, they are reasonably

well suited to the goal of detecting all, or nearly all, of the atomic and molecular emission. The atomic gas is certainly present on much larger physical scales than the molecular gas, but this is compensated to some degree by corresponding differences in beam size. Current heterodyne arrays such as HARP on the JCMT and HERA on the IRAM 30m telescope could be used improve our understanding of beam size effects by mapping the strongest sources in the CO(3-2) and CO(2-1) lines, respectively. At present, though, we have no evidence for a luminosity trend in the relative extent of atomic and molecular gas, and do not anticipate systematic biases introduced by the differences in beam size.

3. RESULTS

3.1. Status of our Search for Cool Gas

The present survey, like our earlier one of lenticular galaxies, differs from previous work in two ways. First, the samples are volume limited, and are not biased towards objects already known or suspected to be gas rich. While Malmquist bias is almost certainly still present, we have reduced it as much as possible given the state of our knowledge of nearby early type field galaxies embodied in the Nearby Galaxies Catalog (Tully 1988) and the Third Reference Catalogue of Bright Galaxies (RC3, de Vaucouleurs et al. (1991)). Second, current understanding of stellar evolution is used to fix sensitivity limits, mandating long integration times for low luminosity galaxies. Our goal in both surveys has been to collect in every case, either from the literature or from new telescope sessions, observations of molecular and atomic gas sufficiently sensitive to detect ~ 1 percent of the gas predicted to be returned by stars during the past 10 Gyr.

One galaxy, Haro 20, still lacks CO observations to our knowledge, while only NGC 4627 has apparently not been searched for atomic hydrogen. We have not attempted to derive an upper limit on the HI content of Maffei 1 from the early, insensitive observation of that galaxy (Spinrad et al. 1971). Because the selection criteria for the present work do not exclude nearby companions (unlike our earlier study of lenticulars) there are a few cases where the low spatial resolution of single-dish observations at 21 cm hinders the attribution of the detected atomic gas to individual galaxies - an important problem when attempting to understand the fate of internally recycled material. Cases of severe confusion include NGC 3226 (Huchtmeier 1994), where nearby NGC 3227 (type Sa) is also in the telescope beam. Likewise, an unknown fraction of the atomic gas found near NGC 7464 (Li & Seaquist 1994) must be attributed to neighboring NGC 7465. We therefore treat NGC 3226 and NGC 7464 as HI non-detections despite the fact that HI has been clearly seen towards both of them. We also exclude those two galaxies when making statistical comparisons with our lenticular

galaxy sample. Finally, we note that NGC 7468, which was briefly discussed in Paper I, continues to stand out for its large quantity of atomic gas.

3.2. Comparisons with Previous Studies

We have located published HI and CO observations of 13 and 8 galaxies, respectively, in the present survey. The majority of the HI overlap comprises objects fainter than $M(B) = -19$, some with early, insensitive observations. The present HI measurements are consistent with published ones in all instances. Improvements in detector technology, and our observational practice of scaling the detection limits with luminosity whenever possible, has resulted new detections or much lower limits on gas content in those cases.

The new CO data are consistent with literature values for the majority of galaxies previously observed; only two cases of disagreement deserve comment. Wiklind et al. (1995) report an IRAM 30m Telescope detection of NGC 4125, finding $I(1-0) = 2.5 \text{ K km s}^{-1}$ (without a stated uncertainty) over a 400 km s^{-1} emission feature. We do not detect that galaxy, measuring $I(1-0) = 0.74 \pm 0.44 \text{ K km s}^{-1}$ by integrating over a similar velocity range. The other case, NGC 4278, has been observed by Combes et al. (2007), who report detecting emission at both $J=1-0$ and $J=2-1$ at roughly 5-sigma using the same telescope but with more sensitive data than ours. We do not confidently detect NGC 4278 in either transition, although the two measurements of $I(1-0)$ are consistent at the combined 1-sigma level. Very recently Crocker et al. (2010) reports that the Plateau de Bure Interferometer has failed to detect $J=1-0$ emission from NGC 4278, setting an upper limit equivalent to 0.49 K km s^{-1} at the 30m Telescope, i.e. roughly 1.6 sigma below our weak detection. It does not appear, therefore, that the $J=1-0$ transition in NGC 4278 has yet been reliably measured. Our upper limit on the $J=2-1$ transition for NGC 4278 is approximately one-third of the 4-sigma measurement published by Combes et al.

3.3. Cool Gas Detection Rates

3.3.1. Global Detection Rates among E and S0 Galaxies

From the volume limited lenticular and elliptical samples (i.e. Welch & Sage (2003), Sage et al. (2007) and the present work) we have distilled subsets classified as E(27 galaxies), E/S0(7), S0(21), S0/Sa(8) or uncertain(10), using classifications from the Carnegie Atlas (Sandage & Bedke 1994) when available, otherwise from the RC3. To reduce the effects of different selection criteria we omit the two elliptical sample members with companions

(see above); all types listed as uncertain are likewise excluded. All further references to morphological type issues in this paper will be to the remaining subsets unless otherwise indicated. We emphasize that they encompass our separate lenticular and elliptical surveys. Detection rates based on those subsets are compared in Table 2 to values calculated by Knapp (1999) from published sources, which are biased to varying degrees towards FIR emission or other signs of abnormality. We caution that the rates for E/S0 galaxies are based on few objects. The tabulated rates for ellipticals are consistent with rates derived from Table 3 after filtering by Carnegie/RC3 type.

Atomic Hydrogen

It is surprising that our surveys detect atomic hydrogen more frequently than previous ones, since Knapp (1999) finds that large IRAS fluxes correlate with increased HI detection rates among early type galaxies. That may simply be due, however, to our efforts to achieve greater sensitivity among fainter galaxies. We find both HI and CO more frequently among lower luminosity galaxies (see below) whereas Table 2 lumps together all luminosities.

Carbon Monoxide

Given the bias of previous studies, the fact that we find a somewhat lower CO detection rate among ellipticals is consistent with the strong correlation between CO and FIR flux in early type galaxies (Knapp 1999). Our detection rate of 26% is essentially the same as the those reported by Knapp and Rupen (1996) from elliptical samples having IRAS 100 micron fluxes of 1.5 Jy or less (their Table 5). We caution against ascribing much significance to that agreement, however, partly because of the luminosity dependence of detection rates. Also, although we omit "uncertain" classifications, the remaining uncertainties in Carnegie/RC3 types could significantly alter the rates in Table 2. Adding all six E/S0 galaxies to type E, for example, would increase HI and CO detection rates to 27% and 64%, respectively.

The present observations are consistent with the result in Paper I that the 30m Telescope more frequently detects CO(2-1) among lenticulars than ellipticals, which was derived by comparing members of our original lenticular and elliptical samples. We focus now on types E, E/S0 and S0 as defined above, and on cases where either or both of the J=1-0 and J=2-1 transitions have been detected at 3σ or higher, and thereby find 2-1 detection rates of 10/10 galaxies = 100% among S0s, 3/3 galaxies = 100% for type E/S0, and 3/5 galaxies = 60% among ellipticals. The statistics of small numbers suggests caution when extrapolating those results. Furthermore, selection effects are present at some level, because the 2-1 spectra from our elliptical survey are a bit noisier than spectra in the same transition from the lenticular

study, thereby lowering detections among ellipticals - recall that our sensitivity requirements are translated into noise limits on J=1-0 spectra.

We point out in Paper I that lower 2-1 detection rates could indicate that ellipticals contain cooler and/or less centrally concentrated molecular gas than S0s. That conclusion, though, is not supported by Figure 2, an update of Figure 2 in Welch & Sage (2003), which compares the intensities in the two transitions.

3.3.2. *The Luminosity Dependence of Detection Rates*

Ignoring possible luminosity differences, the results in Table 2 support the long-held opinion that cool gas is more difficult to find in elliptical galaxies than in lenticulars. Accounting for luminosity reveals the more nuanced perspective shown in Figure 3. Cool gas is indeed much more likely to be found in lenticulars than in ellipticals, but only when comparing luminous galaxies. In contrast, low luminosity objects are very likely to contain detectable amounts of cool gas, be they type E or S0, which is consistent with previous HI (Lake & Schommer 1984) and CO (Lees et al. 1991) surveys. The puzzles, then, are why low luminosity objects are easier to detect, and why gas is found more frequently among luminous early type galaxies with robust disks. We now consider possible explanations.

3.3.3. *Explanations for Variations in Detection Rates*

The trends shown in Figure 3 are unlikely to reflect environmental effects because our selection criteria exclude galaxies within clusters. Likewise our target sensitivities, which scale with absolute luminosity, cannot produce different detection frequencies for samples of similarly luminous galaxies. Early discussions of internal processes which might favor accumulation of cool gas in lower luminosity systems (Faber & Gallagher (1976), Lake & Schommer (1984)) were based on the reasoning that red giant ejecta would, if well mixed, be heated to only modest temperatures because of the small stellar velocity dispersion. The cooling time of such material might therefore be short enough to allow most of it to form dense clouds which would be more difficult for the occasional supernova to push out of the galaxy. Efforts to follow the evolution of red giant outflows (Parriott & Bregman 2008) have focussed on the net effects of energy transfer between the ejected gas and a hot ambient medium without incorporating supernova events. The growth of a central complex of cool gas and dust remains generally plausible. More significant for the question of luminosity effects, though, is that Parriott & Bregman do not find that ejecta from slower moving red giants (i.e. denizens

of less massive galaxies) are able to cool more efficiently. Another possibility, that increased rotational support among low luminosity systems could be linked to higher detection rates, is not supported by the work of Brighenti & Mathews (1997).

We have speculated in Paper I about the role of AGN feedback in the evolution of the cool ISM. A variety of recent theoretical and observational work (e.g. Bower et al. (2006); Kauffmann et al. (2008); Cattaneo et al. (2009); Kormendy et al. (2009)) has raised the possibility that the AGN feedback paradigm, which emerged from efforts to address the cooling flow problem in X-ray galaxy clusters, might be extended to individual galaxy scales. Although many details remain to be worked out, the emerging picture is that cooling at the center of a hot halo stimulates AGN activity. The resulting outflow reheats the halo, cutting off the supply of fuel to the active nucleus and presumably helping destroy clouds of atomic or molecular gas throughout the galaxy. The presence of a massive hot halo, then, decreases the likelihood of finding cool gas. An explanation for the luminosity trend in Figure 3 emerges naturally from such a picture because of the well known scaling relation between the luminosities of X-ray halos and of the stars in the host galaxy (e.g. Canizares (1987); O’Sullivan et al. (2001)). Without enough hot gas to promote AGN feedback, a low luminosity E or S0 galaxy would be more likely to retain cool gas.

How might a disk component give rise to a higher detection rate? One possibility, that supernova explosions are less effective at removing cool gas in flatter galaxies, is not supported by the work of D’Ercole & Ciotti (1998). The AGN feedback paradigm may offer a promising line of attack, because S0 galaxies are significantly dimmer in X-rays than ellipticals of similar luminosity (Eskridge et al. 1995). Therefore, even bright lenticulars perhaps lack the massive hot halos needed to transfer energy to the cool ISM. Furthermore, and regardless of galaxy luminosity, gas returned within a high angular momentum disk environment might be more likely to settle into an extended, dense sheet able to survive heating by surrounding X-ray gas.

It is widely accepted that early type galaxies have formed through a series of mergers. Does the merger paradigm identify what processes might reduce detection rates among more luminous galaxies? Objects resembling field ellipticals emerge in *ab initio* simulations of galaxy formation (Niemi et al. 2010). Although most of the final mass is in place by $z \sim 1$ small amounts continue to fall in thereafter, consistent with the high frequency of disturbance in our combined sample (see below).

A plausible explanation for Figure 3 emerges from simulations (e.g. Naab & Burkert (2003); Gonzalez-Garcia & van Albada (2005); Jesseit et al. (2005); Naab & Trujillo (2006); Naab et al. (2006); Kang et al. (2007)) aimed at identifying the cause of the well-known dichotomy of ellipticals, namely that luminous galaxies are usually rotate slowly and have

boxy isophotes whereas faint ones tend to be rapid rotators with disk-like isophotes. It seems that boxy galaxies are the common outcome of so-called dry (i.e. nearly gas-free, with $M_{gas}/M_{stars} \lesssim 0.1$) mergers, while (wet) mergers of gas-rich disks generate objects resembling elongated, rotationally supported ellipticals or lenticulars. AGN feedback does not play an important role in generating the dichotomy (Kang et al. 2007; Naab et al. 2007). Wet mergers probably spark bursts of star formation, yet since stars form very inefficiently the resulting galaxy would likely contain a significant amount of gas. In the merger paradigm, then, the luminosity trend in Figure 3 could arise because more mergers are needed to build luminous galaxies, but each merger reduces the gas content of the resulting object. In this picture, mergers between a few luminous gas-rich disks could produce modern luminous lenticulars, which would then be expected to contain more gas than their elliptical counterparts. Interestingly, Bois et al. (2010) find that the outcomes of wet merger simulations are strongly resolution-dependent, and such events might after all be able to produce slowly rotating elliptical galaxies. One might then ascribe low detection rates among luminous ellipticals to stellar feedback acting on the cool ISM.

In summary, we believe that both the currently developing paradigms of AGN feedback and the formation of early type galaxies in mergers offer useful insights into the causes of the detection frequencies shown in Figure 3.

3.4. Observational Evidence on the Origin of the Cool Gas in Early Type Galaxies

3.4.1. Cool Gas Masses

One of the most striking results from our earlier lenticular survey (e.g. Figure 12 of Sage & Welch (2006)) is a cutoff of the form $\log[M(\text{obs})] \sim 0.2 \times \log[L_B]$ in the total mass of cool gas present, in which $M(\text{obs}) = 1.4[M(\text{HI}) + M(\text{H}_2)]$ is the observed mass of atomic and molecular gas and L_B is the total blue luminosity. Subsequent work has not clearly confirmed that feature. A similar cutoff was suggested in our preliminary report on the elliptical sample (Figure 2 of Paper I), but is not obvious when the full sample is considered (Figure 4a). On the other hand, an upper cutoff appears to be present in the combined sample (Figure 4b). That impression is greatly enhanced, however, by two galaxies at the low luminosity end of the plot. The current situation, then, is that the cutoff is uncomfortably sample-dependent. Sensitive observations of additional low luminosity galaxies will help settle the question.

We now turn attention to the entire mass range covered by the data. Early work on the distributions of $M(\text{HI})$ (Knapp et al. (1985), Wardle & Knapp (1986)) and, separately,

of $M(\text{H}_2)$ (Lees et al. 1991) in generally FIR-biased samples has uncovered significant differences between E and S0 galaxies, which presumably arise because the two phases originate in different ways in these galaxy types. Does the picture change when comparing volume limited samples? In the spirit of previous investigators we seek to answer that question using the Kaplan-Meier cumulative distribution function (CDF), which is appropriate for samples containing upper limits (Feigelson & Nelson 1985). The value of $\text{CDF}(X)$ is the expected fraction of the sample in which the value of some parameter x is less than X . We have carried out the calculations using two independent software packages: ASURV version 1.3 (Isobe & Feigelson 1990) and R (R Development Core Team 2009), finding essentially the same results. Tests such as log-rank or Kolmogorov-Smirnov are used to compute the likelihood that two CDFs are drawn from the same parent population - the R package employs log-rank and the Peto-Prentice modification of the Wilcoxon test on two censored data sets (Feigelson & Nelson (1985) and references therein).

Figure 5 compares CDFs generated by R for E and S0 galaxies. They are derived from mass estimates alone (left panels) and from masses scaled by the predictions of stellar mass return ($M(\text{pre})$, Ciotti et al. (1991), right panels); the scaling is equivalent to dividing by L_B . In light of earlier work some results are unexpected, and independent of scaling. The CDFs of $M(\text{HI})$ (middle 2 plots), which overlap in places, are likely to have been drawn from the same parent populations with probabilities of 15-20 percent, depending on the method used to compare the two functions. Thus we do not rule out the proposition that E and S0 galaxies have *the same* cumulative mass distributions of atomic hydrogen. That result might in fact be reasonable if we are correct in speculating that much of the HI in both galaxy types has fallen in from a surrounding reservoir. One might then expect the mass of the reservoir and its central galaxy to be at least roughly proportional regardless of optical morphology.

On the other hand, the distributions of $M(\text{H}_2)$ are clearly quite different, especially among higher masses. The probabilities that the two samples come from the same parent population is 2-4 percent. We therefore support the work of Lees et al. (1991) which points toward different evolutionary histories for the molecular ISM components in E and S0 galaxies.

If only the total cool ISM is considered (bottom 2 panels in Figure 5) then the CDFs of E and S0 types are again rather similar, which probably reflects the fact that typically most of the cool ISM is atomic gas. We find probabilities of 8-26 percent that the two cool gas distributions come from the same parent population.

3.4.2. *Molecular to Atomic Gas Mass Ratios*

We have previously (Sage & Welch (2006), Sage et al. (2007)) reported tentative evidence that the mix of atomic and molecular phases in galaxies with increasing amounts of cool gas, be they ellipticals or lenticulars, tends to shift in favour of HI. Adding more data makes the trend, shown in Figure 6, more convincing. Partly because of our decision to use Carnegie/RC3 morphological types, earlier indications of an offset between ellipticals and lenticulars has disappeared. The paucity of data continues to hinder attempts to compare the distributions of molecular to atomic gas mass ratios in Es and S0s. Lees et al. (1991) find no reliable difference between the two distributions, while an analysis similar to that described above returns probabilities of ~ 40 percent that our samples of $M(\text{H}_2)/M(\text{HI})$ have been drawn from the same parent population. More detections are needed before any meaningful difference appears.

Perhaps the most striking aspect of Figure 6 is the presence of two clumps separated by roughly an order of magnitude along both axes. We refer to the clump centered near $M(\text{obs})/M(\text{pre})=0.1$, $M(\text{H}_2)/M(\text{HI})=0.05$ as gas rich, and to the one centred at roughly (0.005, 0.5) as gas poor. Overplotted curves of constant $M(\text{H}_2)/L_B$ and $M(\text{HI})/L_B$ reveal that the separation is mostly caused by differences in HI content. (The outstandingly H_2 -rich outlier near the top of Figure 6 is NGC 3607 whose striking central dusty and CO-rich disk(s?) presents a fascinating challenge for ideas of cool ISM origins (Welch & Sage (2003), Lauer et al. (2005)). The reader will note that the 7 HI non-detections are contained in the gas poor group while all 3 CO non-detections are members of the gas rich clump. We do not believe that fact can be ascribed to significantly different HI and CO sensitivities because achieving similar sensitivities in the two phases has been a goal of our observing strategy (Section 2).

Low luminosity galaxies are known to be relatively gas rich. We search for a possible luminosity difference between clump members by arbitrarily defining the clumps as containing the 17 galaxies towards the top left in Figure 6 (excluding NGC 3607) and the remaining 13 galaxies towards the bottom right, arriving at the memberships shown in Table 4. The two luminosity distributions are shown in Figure 7. Gas rich clump members are indeed fainter by the equivalent of 0.7 magnitude in the mean. The difference, however, is significant at only 1.2 times the combined standard deviation of the means. The Kolmogorov-Smirnov test indicates a probability of 18 percent that the two samples are drawn from the same parent population, which we interpret as only weak support for the hypothesis that the two distributions differ.

3.4.3. *Speculations on the Origin of the Gas*

Differences in global kinematics and morphology motivated our suggestion (Sage & Welch 2006) that internal processes such as cooling flows produce most of the molecular gas we find, while much of the HI has fallen in. Are the results described above at least consistent with those ideas?

An explanation for why ellipticals and lenticulars might share a common CDF for atomic gas but have different CDFs for molecular gas (Figure 5) can be found by returning to our speculation that AGN feedback might produce different detection rates among bright galaxies (Figure 3). We propose that the efficiency of whatever process couples AGN outflow energy to the cool ISM is linked to galaxy type by angular momentum considerations, i.e. a greater tendency for returned (and therefore presumably H₂-rich) gas in lenticular galaxies to settle into highly flattened disks. For example, simple geometry suggests that a highly collimated outflow might not often impact a thin sheet of gas. On the other hand the morphology of the central galaxy might have little connection to the distribution of any infalling gas, which we postulate is mostly HI. In that case the influence of AGN outflows on atomic gas would be similar in Es and S0s, but the outflows would be more effective at removing molecular gas from Es than from S0s.

Merger simulations have not yet attempted to incorporate the conversion of atomic gas into the molecular phase. The merger scenario, however, does offer a plausible explanation for why more gas rich galaxies might also be richer in atomic gas. Suppose galaxies start life imbedded in reservoirs of atomic gas, and that various amounts of this material survives subsequent mergers and blowout due to star formation episodes. Perhaps, then, the gas poor clump comprises galaxies which for some reason have failed to draw down their reservoirs, or whose reservoirs have been removed during successive mergers. Capture of varying amounts of reservoir gas would shift such objects along paths of nearly constant $M(\text{H}_2)/L_B$ towards the lower right in Figure 6. Objects which have captured most nearby gas would join the gas rich clump. It is not clear, though, why reservoir depletion would be the kind of all-or-nothing process needed to produce discrete clumps.

We have searched for other properties besides optical luminosity which might offer clues to the cause of the distribution in Figure 6; references are identified in Table 4. Relevant to the infall scenario, HI interferometer observations have been published for 9 galaxies, and in 8 cases the atomic gas shows evidence of external acquisition; the evidence is equivocal in the case of the ninth galaxy, NGC 7013. Because interferometry requires high column densities it is perhaps not surprising that all but one galaxy (NGC 1052) occupy the gas rich

clump.² More sensitive HI observations of the members of Table 4 are clearly needed.

Returning to optical frequencies, we find that all four galaxies for which published observations suggest previous interactions (e.g. shells, counter rotating stellar components) reside in the gas poor clump. It seems unlikely that the small clump luminosity difference could lead to a selection effect, but we presently have no other explanation for that curious result.

In summary, published observations of Figure 6/Table 4 galaxies are consistent with the merger paradigm in which interactions among early type galaxies are common, and with the notion that capturing various amounts of atomic hydrogen could produce the general trend seen in that figure. They do not appear, however, to point towards an explanation for its bimodal nature.

4. Summary and Conclusions

We present HI and CO observations of a volume limited sample of elliptical galaxies, supplementing the earlier work of Sage et al. (2007) on the same sample (Paper I), and of Welch & Sage (2003) and Sage & Welch (2006) on an analogous group of lenticulars. The observations reported here have generally, but not always, strengthened the trends described in Paper I and in our earlier studies of S0s. We now summarize the most significant results from those three investigations and the present one:

1. We do not clearly confirm our earlier finding of an upper cutoff to the mass of cool gas in early type galaxies (Figures 4a,b). Settling that question will require additional mass estimates for atomic and molecular gas in galaxies with $L_B \lesssim 10^9 L_\odot$ (Figure 4b).
2. Supporting earlier results derived from FIR-biased samples, we find significantly different cumulative mass distributions for *molecular* gas in E and S0 galaxies (Figure 5). Contrary to previous work, however, we do not rule out the hypothesis that the cumulative distributions of *atomic* gas are the same.
3. More gas rich early type galaxies have lesser proportions of molecular gas (Figure 6). The ratio of molecular to atomic gas mass $M(\text{H}_2)/M(\text{HI})$ varies by roughly two orders of magnitude, from ~ 5 for extremely gas poor systems to ~ 0.05 for the most gas rich ones.

²Interestingly, both the HI and CO emission from the dwarf S0 NGC 404, a gas rich clump member, have been mapped by del Rio et al. (2004) and Taylor & Petitpas (2004), respectively. In contrast to the atomic gas, which is found beyond 100'' from the center of the galaxy, the CO occupies only the inner 9'', consistent with our speculation that most of the molecular gas comes from stellar mass return.

Surprisingly, the variation manifests itself as clumping around quite different combinations of gas content and molecular mass fraction. We are presently unable to identify a reason for this striking result.

4. We extend previous work which shows that cool gas is generally easier to find in S0s than ellipticals, by demonstrating that the effect appears primarily among luminous galaxies (Figure 3). Low luminosity objects of either type are likely to contain detectable quantities of cool gas.

Our surveys of E and S0 galaxies provide a general picture of cool gas in early type galaxies in low density environments, which is largely free of the biases present in earlier work. We have explored for the first time the relationship between the two gas phases across a wide range of ISM mass, with results which challenge current ideas of ISM evolution. We speculate on how some of our findings might be explained, finding that both the AGN feedback and merger paradigms offer attractive possibilities. From an observational perspective the central and obvious obstacle to better understanding remains low sensitivity. Despite generous grants of telescope time we have still not glimpsed the cool gas within even most bright ellipticals. Many detections are weak, and the maps required to fully account for gas missed by single pointing observations are not yet available. Finding the gas, and charting its morphology and kinematics across a wide range of optical luminosity, will be the task of the next generation of radio telescopes. Only by taking on that task can we hope to answer the fundamental question of how internal processes compete with external ones to shape what we see. At present the greatest certainties remain the ones which motivated our surveys: Stars in E and S0 galaxies have returned much more gas than has been found, and additional gas sometimes falls in from outside.

This work has been supported by a Discovery Grant to Welch from the Natural Sciences and Engineering Research Council of Canada. Young acknowledges funding by NSF AST-0507432. We thank the referee for several comments which helped us to improve our presentation.

Facilities: IRAM:30m, GBT

REFERENCES

- Barth, A. J., Ho, L. C., Filippenko, A. V., & Sargent, W. L. W. 1998, ApJ, 496, 133
- Bertola, F., Buson, L. M., & Zeilinger, W. W. 1992, ApJ, 401, L79
- Bois, M. et al. 2010, MNRAS, accepted

- Bower, R. G., et al. 2006, MNRAS, 370, 645
- Bregman, J. N., Hogg, D. E., & Roberts, M. S. 1992, ApJ, 387, 484
- Braine, J., Henkel, C., & Wiklind, T. 1997, A&A, 321, 765
- Brighenti, F., & Mathews, W. G. 1997, ApJ, 490, 592
- Canizares, C. R., Fabbiano, G., & Trinchieri, G. 1987, ApJ, 312, 503
- Cattaneo, A., et al. 2009 Nature, 460, 213
- Ciotti, L., D’Ercole, A., Pellegrini, S., & Renzini, A. 1991, ApJ, 376, 380
- Combes, F., Young, L. M., & Bureau, M. 2007, MNRAS, 377, 1795
- Crocker, A. F., Bureau, M., Young, L. M., & Combes, F. 2010, MNRAS, submitted
- del Rio, M. S., Brinks, E., & Cepa, J. 2004, AJ, 128, 89
- D’Ercole, A., & Ciotti, L. 1998, ApJ, 494, 535
- de Vaucouleurs, G., de Vaucouleurs, A., Corwin, H. G., Buta, R. J., Paturel, G., & Fouque, P. 1991, Third Reference Catalogue of Bright Galaxies, Version 3.9 (New York:Springer-Verlag) [RC3]
- Emsellem, E., et al. 2004, MNRAS, 352, 721
- Eskridge, P. B., Fabbiano, G., & Kim, D.-W. 1995, ApJS, 97, 141
- Faber, S., & Gallagher, J. S. 1976, ApJ, 204, 365
- Feigelson, E. D., & Nelson, P. I. 1985 ApJ, 293, 192
- Fisher, D. 1997, AJ, 113, 950
- Gonzalez-Garcia, A. C. & van Albada, T. S. 2005, MNRAS, 361, 1043
- Goudfrooij, P., de Jong, T., Hansen, L., & Norgaard-Nielsen, H. U. 1994, MNRAS, 271, 833
- Huchtmeier, W. K., Sage, L. J., & Henkel, C. 1995, A&A, 300, 675
- Huchtmeier, W. K. 1994, A&A, 268, 389
- Isobe, T., & Feigelson, E. D. 1990, BAAS, 22, 917
- Irwin, J. A., Seaquist, E. R., Taylor, A. R., & Duric, N. 1987, ApJ, 313, L91

- Jesseit, R., Naab, T. & Burkert, A. 2005, MNRAS, 360, 1185
- Kang, X., van den Bosch, F. C. & Pasquali, A. 2007, MNRAS, 381, 389
- Kauffmann, G., Heckman, T. M., & Best, P. M. 2008, MNRAS, 384, 953
- Kim, D.-W. 1989, ApJ, 346, 653
- Knapp, G. R., Kerr, F. G., & Henderson, A. P. 1979, ApJ, 234, 448
- Knapp, G. R., van Driel, W., Schwarz, U. J., van Woerden, H., & Gallagher, J. S. III 1984, A&A, 133, 127
- Knapp, G. R., Turner, E. L., & Cunniffe, P. E. 1985, AJ, 90, 454
- Knapp, G. R., & Rupen, M. P. 1996, ApJ, 460, 271
- Knapp, G. R. 1999, in Cold Gas and Star Formation in Elliptical Galaxies, ASP Conference Series 163, eds. J. Sepa and P. Carral (San Francisco: ASP), 119
- Kormendy, J., Fisher, D. B., Cornell, M. E., & Bender, R. 2009, ApJS, 182, 216
- Kumar, C. K., & Thonnard, N. 1983, AJ, 88, 260
- Lake, G., & Schommer, R. A. 1984, ApJ, 280, 107
- Lake, G., Schommer, R. A. & van Gorkom, J. H. 1987, ApJ, 314, 57
- Lauer, T. R., Faber, S. M., & Gebhardt, K., 2005, AJ, 129, 2138
- Lees, J., Knapp, G. R., Rupen, M. P., & Phillips, T. G. 1991, ApJ, 379, 177
- Li, J. G., & Seaquist, E. R. 1994, AJ, 107, 1953
- Morganti, R., et al. 2006, MNRAS, 371, 157
- Naab, T. & Burkert, A. 2003, ApJ, 597, 893
- Naab, T. & Trujillo, I. 2006, MNRAS, 369, 625
- Naab, T., Jesseit, R. & Burkert, A. 2006, MNRAS, 372, 839
- Naab, T., Johansson, P. H., Ostriker, J. P. & Efstathiou, G. 2007, ApJ, 658, 710
- Niemi, S.-M., Heinamaki, P. & Saar, E. 2010, MNRAS, 405, 477

- Oosterloo, T., Morganti, R., Sadler, E. M., van der Hulst, T., & Serra, P. 2007, *A&A*, 465, 787
- O’Sullivan, E., Forbes, D., & Ponman, T. 2001, *MNRAS*, 328, 461
- Parriott, J. R., & Bregman, J. N. 2008, *ApJ*, 681, 1215
- Prugniel, P., Nieto, J.-L., Davoust, E., & Bender, R. 1988, *A&A*, 204, 61
- R Development Core Team. 2009, *R: A Language and Environment for Statistical Computing* (Vienna: R Foundation for Statistical Computing) <http://www.R-project.org>
- Raimond, E., Faber, S. M., Gallagher, J. S. III, & Knapp, G. R. 1981, *ApJ*, 246, 708
- Sage, L. J., & Welch, G. A. 2006, *ApJ*, 644, 850
- Sage, L. J., Welch, G. A., & Young, L. M. 2007, *ApJ*, 657, 232 (Paper I)
- Sancisi, R., van Woerden, H., Davies, R. D., & Hart, L. 1984, *MNRAS*, 210, 497
- Sandage, A., & Bedke, J. 1994, *The Carnegie Atlas of Galaxies* (Washington, DC: Carnegie Institution)
- Shostak, G. S. 1987, *A&A*, 175, 4
- Spinrad, H., et al. 1971, *ApJ*, 163, L25
- Springob, C. M., Haynes, M. P., Giovanelli, R., & Kent, B. R. 2005, *ApJS*, 160, 149
- Taylor, C. L., & Petitpas, G. R. 2004, *BAAS*, 36, 1492
- Tully, R.B. 1988, *Nearby Galaxies Catalog*, (Cambridge: Cambridge University Press)
- van Driel, W. van Woerden, H., Gallagher, J. S. III, & Schwarz, U, J. 1988, *A&A*, 191, 201
- van Gorkom, J. H., Knapp, G. R., Raimond, F., Faber, S. M., & Gallagher, J. S. 1986, *AJ*, 91, 791
- Walsh, D. E. P., van Gorkom, J. H., Bies, W. E., Katz, N., Knapp, G. R., & Wallington, S. 1990, *ApJ*, 352, 532
- Wardle, M., & Knapp, G. R. 1986, *AJ*, 91, 23
- Welch, G. A., & Sage, L. J. 2003, *ApJ*, 584, 260

- Whitmore, B. C., Lucas, R. A., McElroy, D. B., Steiman-Cameron, T. Y., Sackett, P. D. & Olling, R. P. 1990, *AJ*, 100, 1489
- Wiklind, T., Combes, F., & Henkel, C. 1995, *A&A*, 297, 643
- Williams, B. A., McMahon, P. M., & van Gorkom, J. H. 1991, *AJ*, 101, 1957
- Young, L. M. 2002 *AJ*, 124, 788
- Young, L. M. 2005 *ApJ*, 634, 258
- Young, L. M., Bureau, M., & Cappellari, M. 2008, *ApJ*, 676, 317

Table 1. Integrated Intensities

Name	Window (km s ⁻¹)	I _{CO} (1-0) (K km s ⁻¹)	rms (K)	I _{CO} (2-1) (K km s ⁻¹)	rms (K)	I _{HI} (K km s ⁻¹)	rms (K)
NGC 584	1585-2019	1.59 ± 0.72	0.0088	1.57 ± 1.42	0.0173	< 0.31	0.0058
NGC 596	1725-2027	< 0.61	0.0097	4.24 ± 1.38	0.0221
NGC 636	1704-2016	< 0.26	0.0059
NGC 720	1498-1992	< 0.40	0.0072
NGC 821	1541-1920	0.59 ± 0.32	0.0044	< 0.52	0.0071
IC 225	1508-1591	0.037	0.0024
NGC 1052	1180-1700	< 0.93	0.0097	7.72 ± 1.67	0.0175
NGC 1172	1548-1790	0.85 ± 0.39	0.0071	< 0.48	0.0086	< 0.18	0.0047
NGC 1297	1469-1687	< 0.34	0.0067	0.43 ± 0.41	0.0081	< 0.16	0.0045
Haro 20	1740-1950	3.76 ± 0.11	0.0033
NGC 1407	1493-2064	< 0.31	0.0050
NGC 3115 DW1	665-731	< 0.040	0.0021
NGC 3156	1206-1430	0.59 ± 0.06	0.0016
NGC 3226	986-1246	0.90 ± 0.30	0.0052	1.02 ± 0.44	0.0076
NGC 3377	534-796	0.32 ± 0.30	0.0051	< 0.70	0.0120
NGC 3379	710-1112	< 0.41	0.0052	< 0.93	0.0119
UGC 5955	1177-1321	0.38 ± 0.14	0.0035	0.45 ± 0.20	0.0049	< 0.040	0.0017
NGC 3522	1050-1400	< 0.16	0.0023	0.34 ± 0.28	0.0038
IC 678	834-1101	0.28 ± 0.14	0.0047	1.13 ± 0.52	0.0087	< 0.040	0.0017
NGC 3640	1075-1427	< 0.53	0.0077	2.04 ± 0.61	0.0088
NGC 3818	1495-1963	1.48 ± 0.85	0.0097	< 0.70	0.0080	< 0.20	0.0038
NGC 4033	1491-1743	< 0.53	0.0096	< 0.65	0.0116	< 0.087	0.0023
NGC 4125	1127-1585	0.74 ± 0.44	0.0053	2.30 ± 0.95	0.0113	< 0.18	0.0034
NGC 4239	848-1032	< 0.051	0.0016
UGC 7354	1489-1640	0.50 ± 0.17	0.0041	1.13 ± 0.24	0.0058
NGC 4278	383-915	1.52 ± 0.63	0.0066	< 0.78	0.0082
NGC 4308	501-677	0.28 ± 0.13	0.0028	0.40 ± 0.20	0.0044
UGC 7767	1125-1337	< 0.22	0.0040	1.45 ± 0.38	0.0070	2.17 ± 0.14	0.0037
NGC 4648	1193-1635	< 0.20	0.0037
NGC 4627	435-597	0.30 ± 0.25	0.0058	0.96 ± 0.31	0.0072

Table 1—Continued

Name	Window (km s ⁻¹)	I _{CO} (1-0) (K km s ⁻¹)	rms (K)	I _{CO} (2-1) (K km s ⁻¹)	rms (K)	I _{HI} (K km s ⁻¹)	rms (K)
UGCA 298	769-901	0.38 ± 0.19	0.0046	2.15 ± 0.36	0.0089	1.25 ± 0.08	0.0030
NGC 4697	1076-1406	< 0.22	0.0049
NGC 4742	1177-1363	0.117 ± 0.048	0.0041
NGC 5845	1199-1701	0.43 ± 0.38	0.0041	< 0.51	0.0055	< 0.12	0.0021
NGC 7464	1777-1972	0.55 ± 0.27	0.0054	0.72 ± 0.41	0.0083

Note. — Columns contain the galaxy name, location of line window, and for both CO lines and HI, the integrated line intensity in the line window and its formal standard deviation along with rms channel noise in the smoothed spectrum. The temperature scales are T_{mb} and T_A for CO and HI, respectively. All upper limits are 1σ and they are used whenever the formal line intensity is less than 1σ . Observations for many of the galaxies without values were reported in Paper I.

Table 2. Cool Gas Detection Rates

Type	Atomic Hydrogen					Molecular Gas			
	Present		Knapp			Present		Knapp	
	percent	N	percent	N		percent	N	percent	N
E	19	27	5	64	...	26	27	39	61
E/S0	67	6	17	23	...	67	6	31	26
S0	57	21	20	103	...	62	21	47	43

Note. — Columns list morphological type from Sandage & Bedke (1994) when available, otherwise from de Vaucouleurs et al. (1991), and the percent of galaxies detected in our combined S0 and elliptical surveys or listed by Knapp (1999) out of a total of N galaxies. Columns 2-5 concern HI detections, while CO detections are summarized in columns 7-10.

Table 3. Total Cool Gas Masses

Name	Type	M(H ₂) (M_{\odot})	M(HI) (M_{\odot})	H ₂ reference	HI reference
NGC 584	S0 1 (3,5)	$< 5.15 \times 10^7$	$< 5.95 \times 10^7$	2	2
NGC 596	E0/S0 1 (disk)	3.72×10^7	1.45×10^8	2	3
NGC 636	E1	$< 1.67 \times 10^7$	$< 5.30 \times 10^7$	1	2
NGC 720	E5	$< 2.40 \times 10^7$	$< 5.88 \times 10^7$	1	2
NGC 821	E6	$< 2.23 \times 10^7$	$< 3.09 \times 10^8$	2	3
NGC 855	[E]	7.45×10^5	2.68×10^7	4	5
IC 225	[E]	2.50×10^6	$< 3.82 \times 10^6$	1	2
Maffei 1	[gE]	$< 2.08 \times 10^5$	\dots^a	1	6
NGC 1052	E3/S0 1(3)	3.78×10^7	4.53×10^7	2	5
NGC 1172	S0 1(0,3)	$< 1.70 \times 10^7$	$< 2.09 \times 10^7$	2	2
NGC 1297	S0 2/3(0)	$< 1.50 \times 10^7$	$< 1.91 \times 10^7$	2	2
Haro 20	[E+ (doubtful)]	\dots	2.13×10^8	\dots	2
NGC 1407	[E0]	$< 3.35 \times 10^7$	$< 1.52 \times 10^8$	1	2
NGC 2768	S0 1/2(6)	4.99×10^7	1.98×10^8	1	5
NGC 3073	[SAB0-]	7.68×10^6	1.66×10^8	1	7
NGC 3115 DW 1	[dE1, N]	$< 3.33 \times 10^6$	$< 2.55 \times 10^6$	1	2
NGC 3156	E5/S0 2/3(5)	3.32×10^7	2.41×10^7	8	2
NGC 3193	E2	$< 4.46 \times 10^7$	$< 7.98 \times 10^7$	1	9
NGC 3226	E2/S0 1(2)	2.14×10^7	\dots^b	2	3
NGC 3377	E6	$< 2.51 \times 10^6$	$< 4.17 \times 10^6$	2	10
NGC 3379	E0	$< 3.48 \times 10^6$	$< 2.78 \times 10^6$	2	11
UGC 5955	[E]	$< 5.28 \times 10^6$	$< 3.99 \times 10^6$	2	2
NGC 3522	[E]	$< 5.48 \times 10^6$	1.08×10^8	2	12
IC 678	[E]	$< 5.61 \times 10^6$	$< 4.36 \times 10^6$	2	2
NGC 3605	E5	$< 1.43 \times 10^7$	$< 2.39 \times 10^7$	1	10

Table 3—Continued

Name	Type	M(H ₂) (M_{\odot})	M(HI) (M_{\odot})	H ₂ reference	HI reference
NGC 3608	E1	$< 1.02 \times 10^8$	$< 3.48 \times 10^7$	8	12
NGC 3640	[E3]	1.85×10^7	$< 7.44 \times 10^7$	2	12
NGC 3818	E5	$< 6.70 \times 10^7$	$< 4.30 \times 10^7$	2	2
NGC 4033	S0 1(6)	$< 3.96 \times 10^7$	$< 1.46 \times 10^7$	2	2
NGC 4125	E6/S0 1/2(6)	$< 3.38 \times 10^7$	$< 3.67 \times 10^7$	2	2
NGC 4239	[E]	$< 9.89 \times 10^6$	$< 4.93 \times 10^6$	1	2
UGC 7354	[E pec (unc)]	3.73×10^6	1.01×10^8	2	5
NGC 4278	E1	$< 7.65 \times 10^6$	2.59×10^8	2	13
NGC 4283	E0	3.41×10^6	4.15×10^7	1	3
NGC 4308	[E (unc)]	$< 8.68 \times 10^5$	$< 1.13 \times 10^7$	2	12
NGC 4494	E1	5.59×10^6	$< 9.96 \times 10^6$	1	11
UGC 7767	[E]	7.20×10^6	8.18×10^7	2	2
NGC 4648	[E3]	$< 1.60 \times 10^7$	$< 2.69 \times 10^7$	1	2
NGC 4627	dE5, N	2.79×10^6	...	2	...
NGC 4636	E0/S0 1(6)	$< 7.15 \times 10^6$	$< 6.12 \times 10^7$	1	14
UGCA 298	[E+ (unc)]	2.63×10^6	1.16×10^7	2	2
NGC 4697	E6	$< 2.96 \times 10^7$	$< 4.22 \times 10^7$	1	2
NGC 4742	E4	$< 1.40 \times 10^7$	$< 2.54 \times 10^7$	1	2
NGC 5845	[E (unc)]	$< 2.37 \times 10^7$	$< 2.07 \times 10^7$	2	2
NGC 7464	[E1 pec (unc)]	$< 1.29 \times 10^7$... ^c	2	15
NGC 7468	[E3 pec (unc)]	2.35×10^7	1.59×10^9	1	5

Note. — Columns contain galaxy name, morphological type from the Carnegie Atlas or RC3 (square brackets), H₂ mass or upper limit, HI mass or upper limit, source of H₂ value, source of HI value. Upper limits are 3σ , and results derived by other observers have been corrected to the distances in Paper I. A CO-to-H₂ conversion factor of 2.3×10^{20} mol. cm⁻² (K km s⁻¹)⁻¹ has been used.

^aMaffei 1: An early HI observation (Spinrad et al. 1971) is too insensitive to be useful.

^bNGC 3226: Published HI measurement confused by NGC 3227 (type Sa).

^cNGC 7464: Published HI observations confused by NGC 7565.

References. — (1) Paper I; (2) present work; (3) Huchtmeier (1994); (4) Wiklind et al. (1995); (5) Huchtmeier et al. (1995); (6) Spinrad et al. (1971); (7) Irwin et al. (1987); (8) Combes et al. (2007); (9) Williams et al. (1991); (10) Knapp et al. (1979); (11) Bregman et al. (1992); (12) Lake & Schommer (1984) (13) Raimond et al. (1981); (14) Kumar & Thonnard (1983); (15) Springob et al. (2005).

Table 4. Figure 6 Clump Members

Gas-Rich			Gas-Poor		
Name	Type	Reference	Name	Type	Reference
NGC 404	S0	1	NGC 596	E/S0	12
NGC 855	E	2	IC 225	E	...
NGC 1023	S0	3, 4	NGC 1052	E/S0	13
NGC 2787	S0/a	5	NGC 2768	S0	14, 15
NGC 3073	S0	6	NGC 3115	S0	...
NGC 3522	E	...	NGC 3156	E/S0	...
NGC 3870	S0	7	NGC 3384	S0	16
NGC 3941	S0/a	8	NGC 3412	S0	...
NGC 4203	S0	9	NGC 3489	S0/a	...
NGC 4278	E	10	NGC 3640	E	17
NGC 4283	E	...	NGC 4026	S0	...
UGC 7767	E	...	NGC 4111	S0	18
NGC 7013	S0/a	11	NGC 4150?	S0/a	19
...	NGC 4494	E	...
...	NGC 4880	E/S0	...
...	NGC 5866?	S0	...
...	NGC 7457	S0	19

Note. — Broad morphological types, taken from the Carnegie Atlas or RC3, are listed for members of the two clumps in Figure 6. NGC 3607, near the top of the plot, is excluded; question marks indicate other outliers which might be excluded. References point to data suggesting past interactions such as extended and/or misaligned HI, optical shells, counterrotating stars or gas, polar rings - 1: del Rio et al. (2004), 2: Walsh et al. (1990), 3: Sancisi et al. (1984), 4: Morganti et al. (2006), 5: Shostak (1987), 6: Irwin et al. (1987), 7: Sage & Welch (2006), 8: Fisher (1997), 9: van Driel et al. (1988), 10: Raimond et al. (1981), 11: Knapp et al. (1984), 12: Goudfrooij et al. (1994), 13: van Gorkom et al. (1986), 14: Kim (1989), 15: Bertola (1992), 16: Whitmore et al. (1990), 17: Prugniel et al. (1988), 18: Barth et al. (1998), 19: Emsellem et al. (2004)

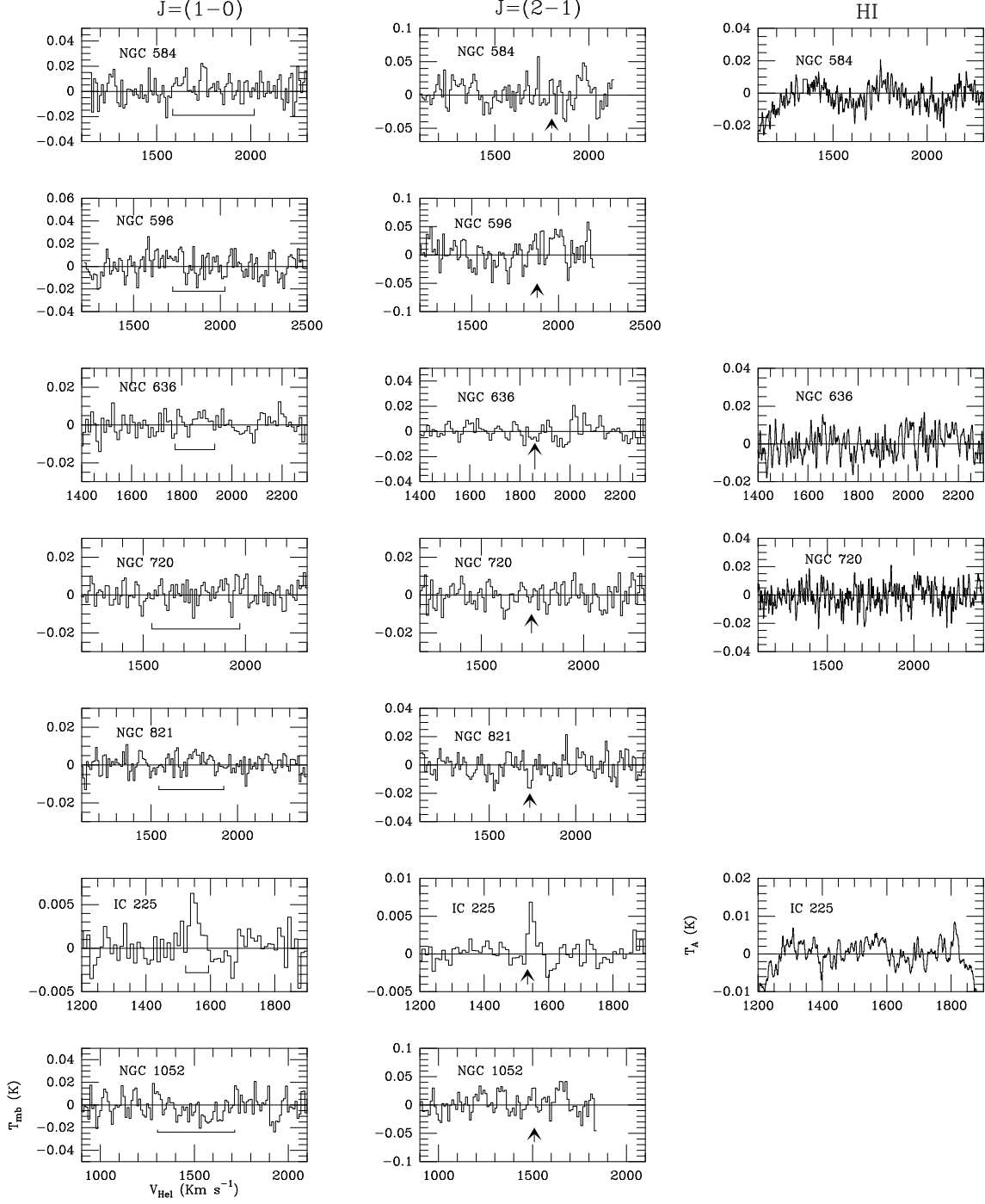
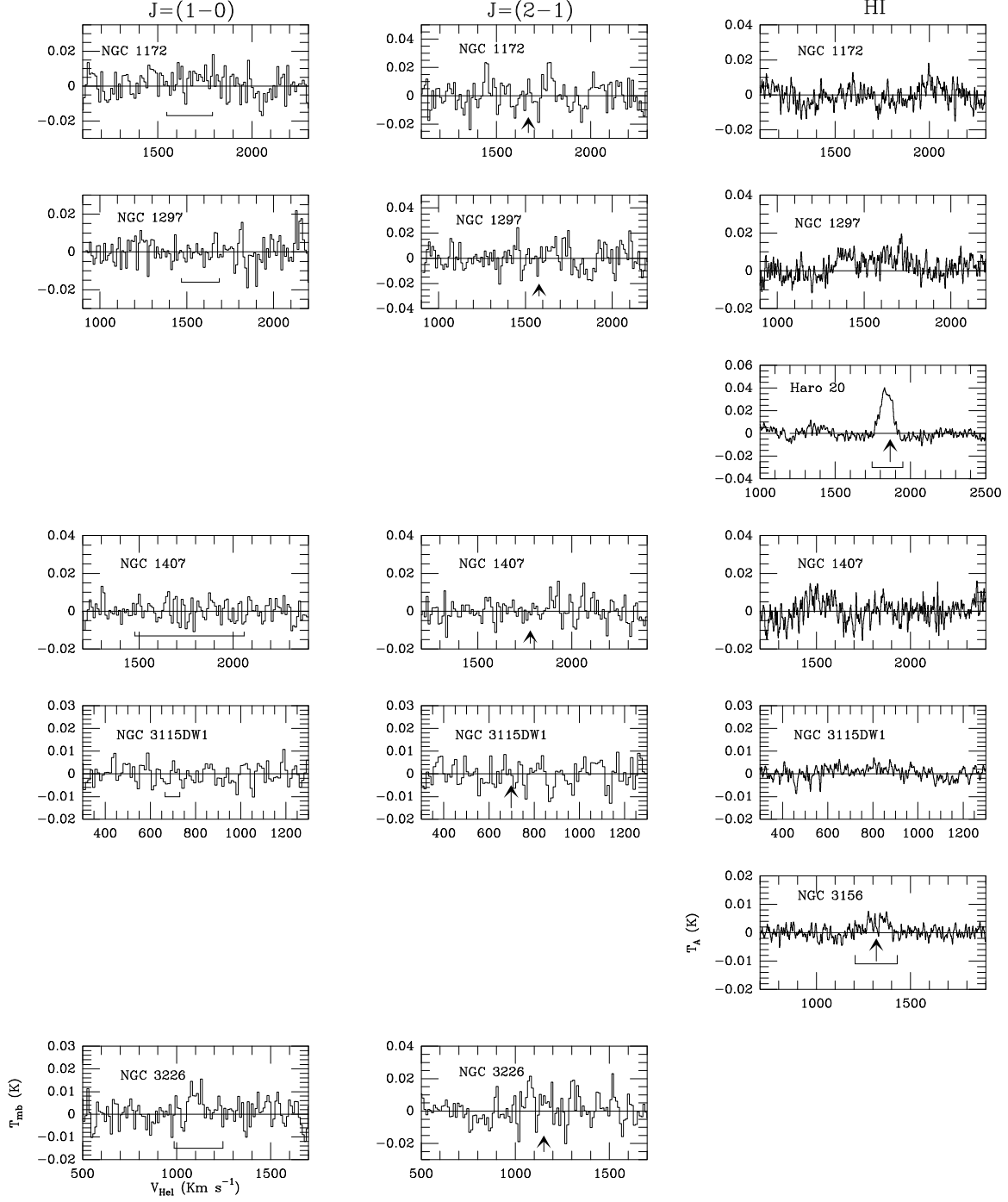
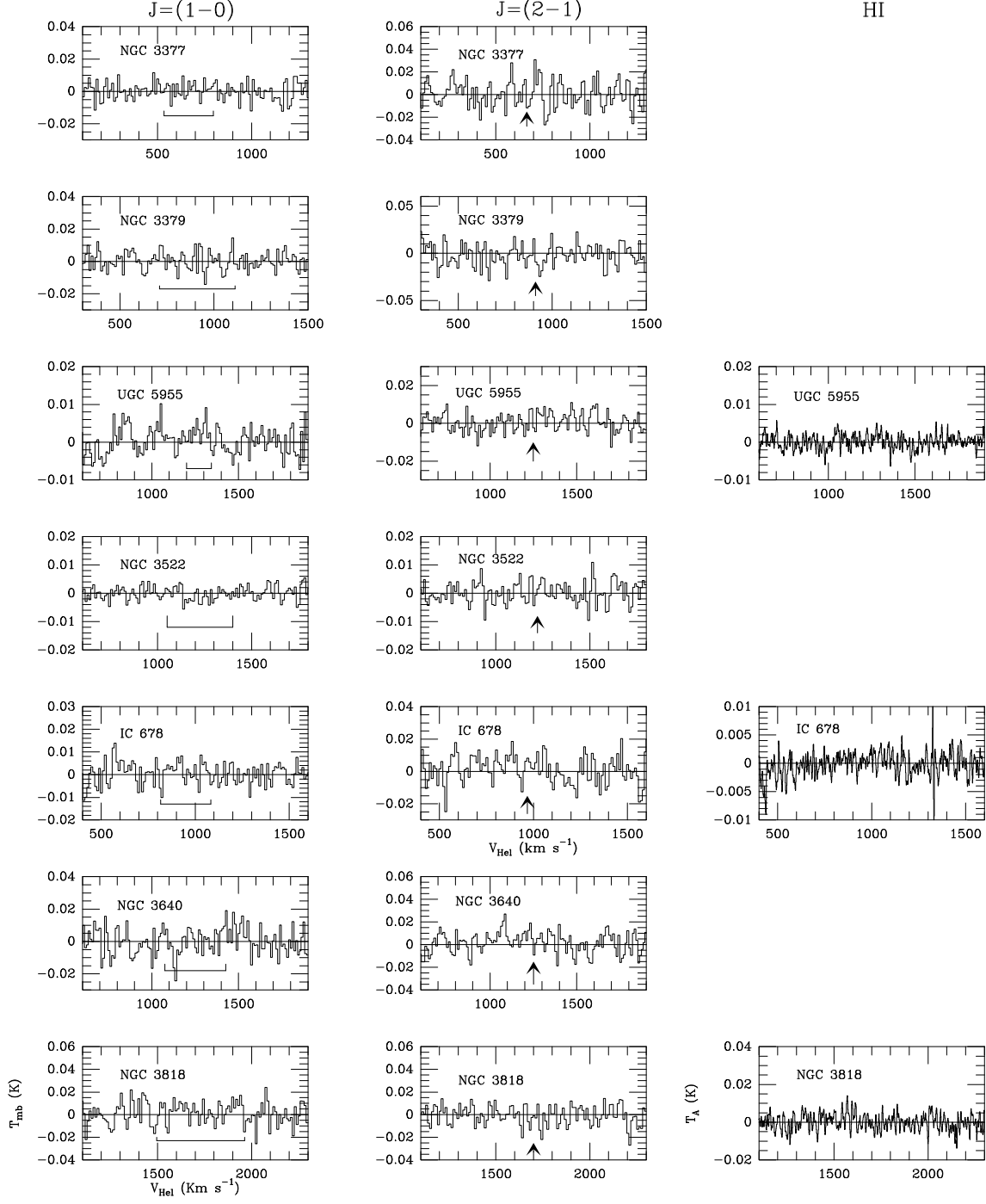
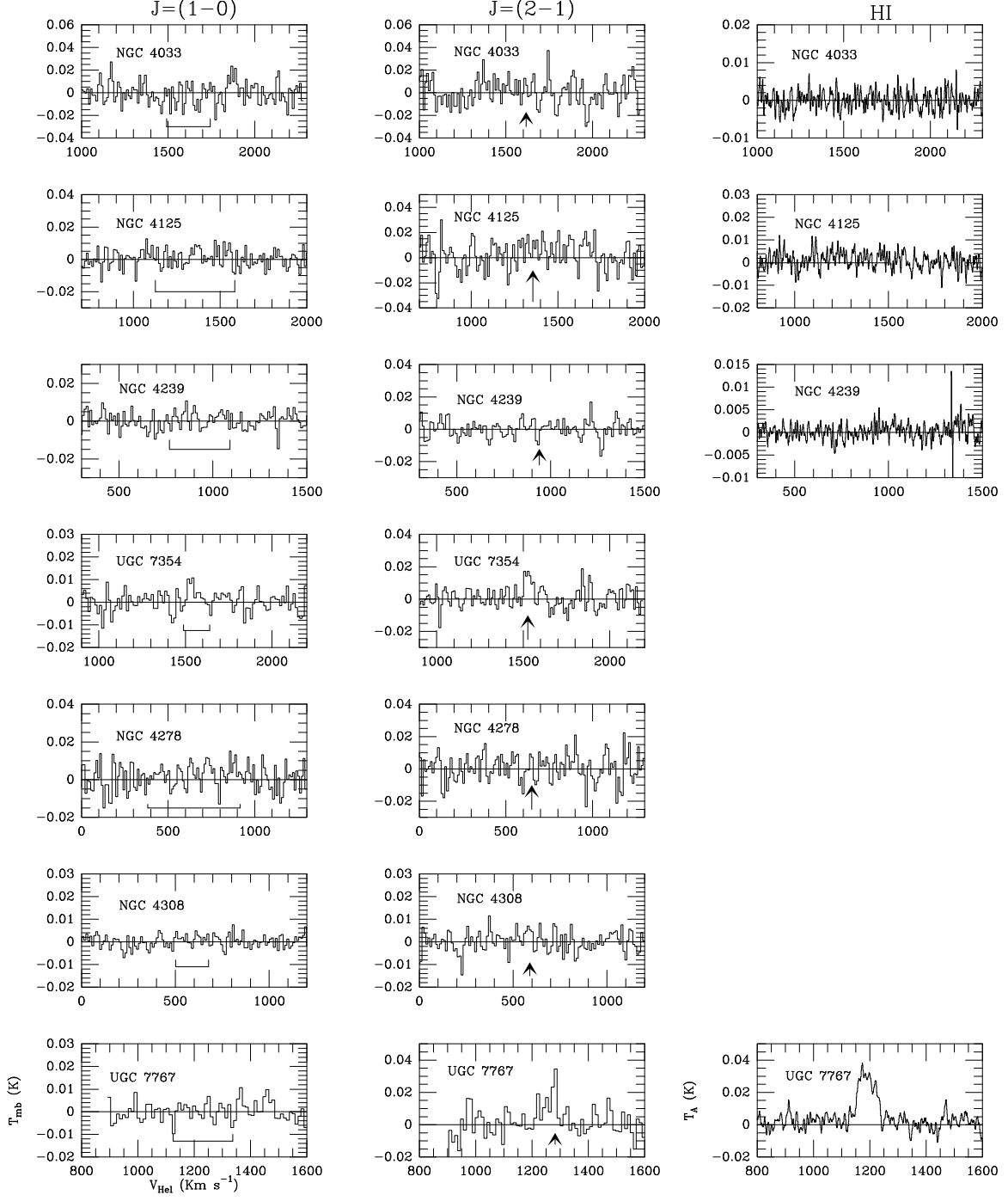
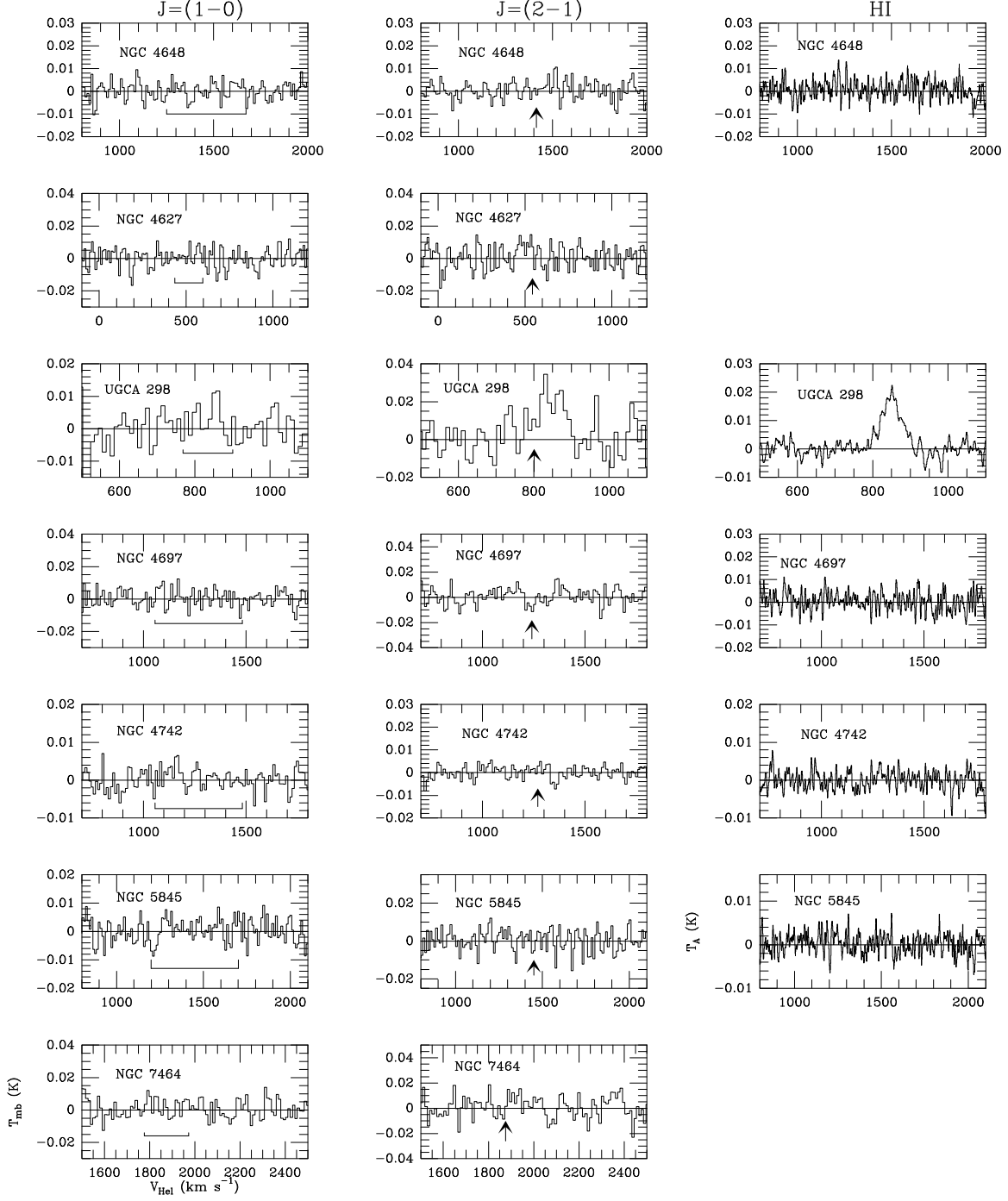


Fig. 1a.— CO and HI spectra from the IRAM 30m telescope and the GBT, respectively. Arrows indicate the optical systemic velocity from NED, and horizontal lines show the velocity range over which the integrated line intensity was calculated in all spectra.









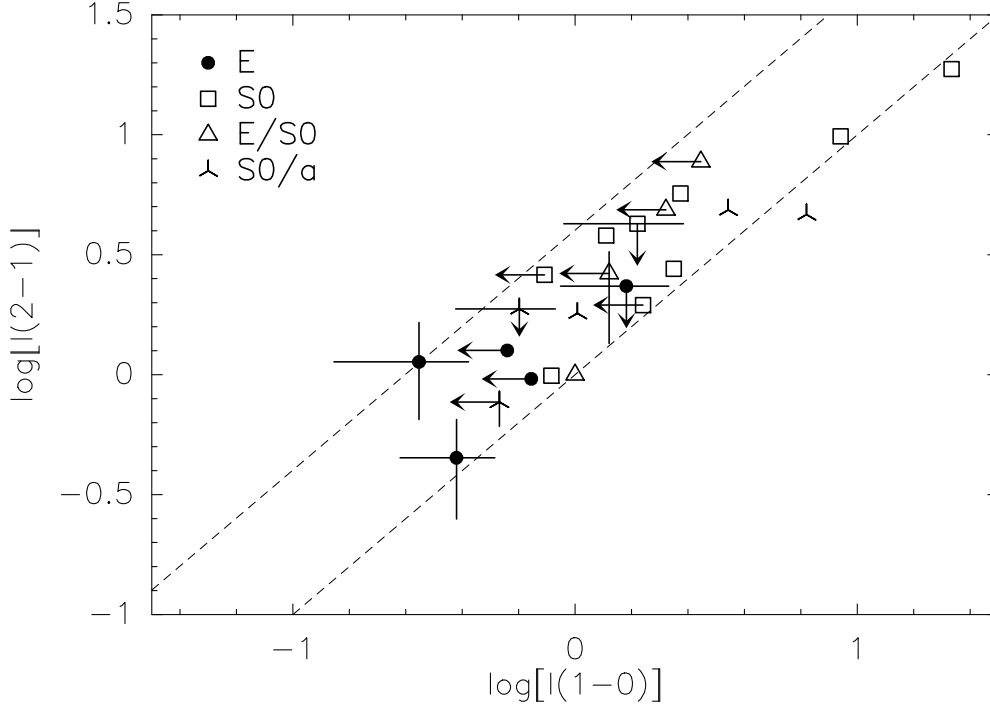


Fig. 2.— Integrated CO intensities for galaxies detected in one or both indicated transitions at the 30m Telescope. Morphological classifications are from the Carnegie Atlas (Sandage & Bedke 1994) or the RC3 (de Vaucouleurs et al. 1991). Error bars have full lengths of 2σ ; and are comparable to the size of the plotted point if not shown. Each non-detection is plotted at the 3σ value of the non-detected transition with an arrow extending to the 2σ value. Dashed lines indicate the relationships for point sources (top line) or those which are uniform across both beams. This plot updates Figure 2 of Welch & Sage (2003).

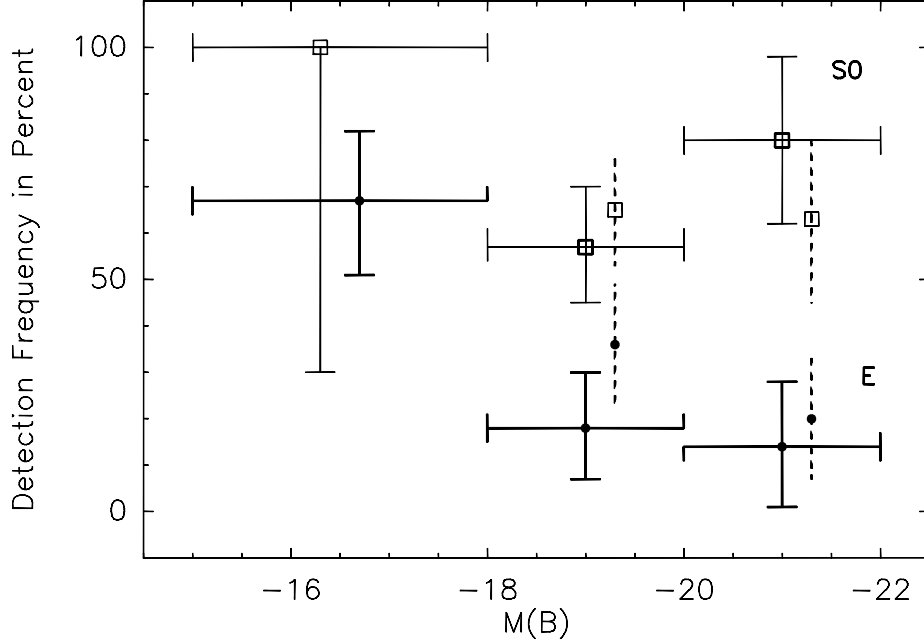


Fig. 3.— Percent of galaxies with different absolute blue magnitudes which are detected in at least one of HI or CO. Morphological types are from the Carnegie Atlas or RC3. Horizontal bars indicate bin sizes. Vertical error bars show 1-sigma uncertainties computed assuming that detections follow a Binomial Distribution with detection probability given by the ratio of the number of detections to the total number in the bin. Error bars for the faintest S0 galaxies, however, are based on the square root of the number of detections; there are only 2 S0 galaxies in the lowest luminosity bin and both are detected. Small horizontal offsets are applied to separate Es and S0s in the faintest bin. Type E/S0 is not shown separately because it includes only 6 galaxies. Offset symbols with dashed error bars show how the E or S0 data points would change if all 6 E/S0 galaxies were to be assigned to one of those types; no E/S0 galaxies would be included in the faintest bin.

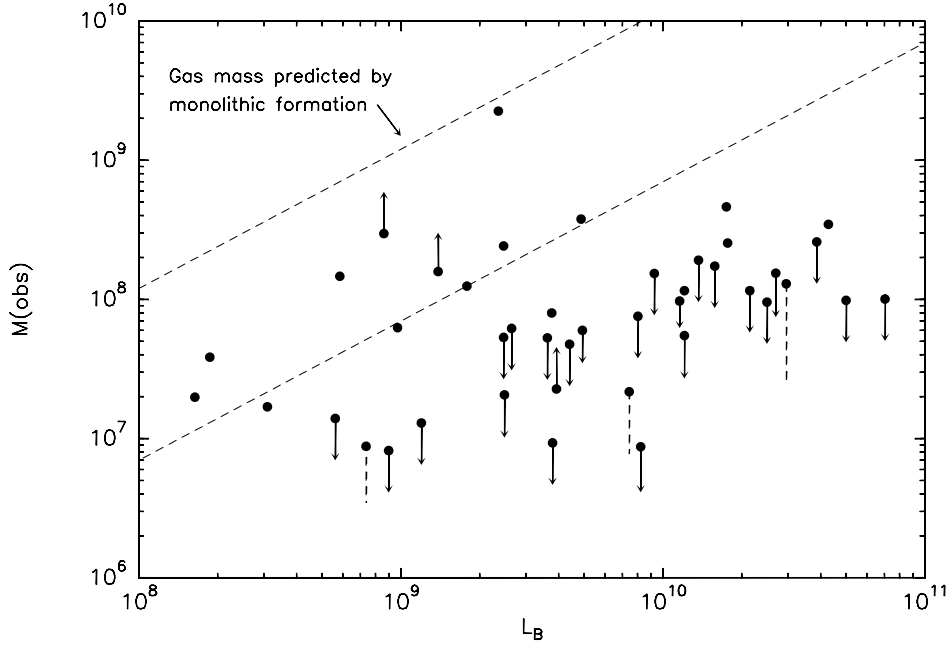


Fig. 4a.— The observed mass of cool gas versus blue luminosity among galaxies in the elliptical sample, plotted to compare directly with results for our lenticular sample (Figure 12 of Sage & Welch (2006)). Dashed lines connect the sum of an observation and 3-sigma limit (point) to the observation alone. Down arrows extend from the sum of 3-sigma upper limits on HI and H₂ masses, whereas up arrows identify HI detections without CO observations. Inclined dashed lines show the predictions of the analytical approximation of Ciotti et al. (1991) for gas returned in a 10 Gyr old stellar population after the first 0.5 Gyr (top), and the estimate of Faber & Gallagher (1976) for only solar type stars over 10 Gyr.

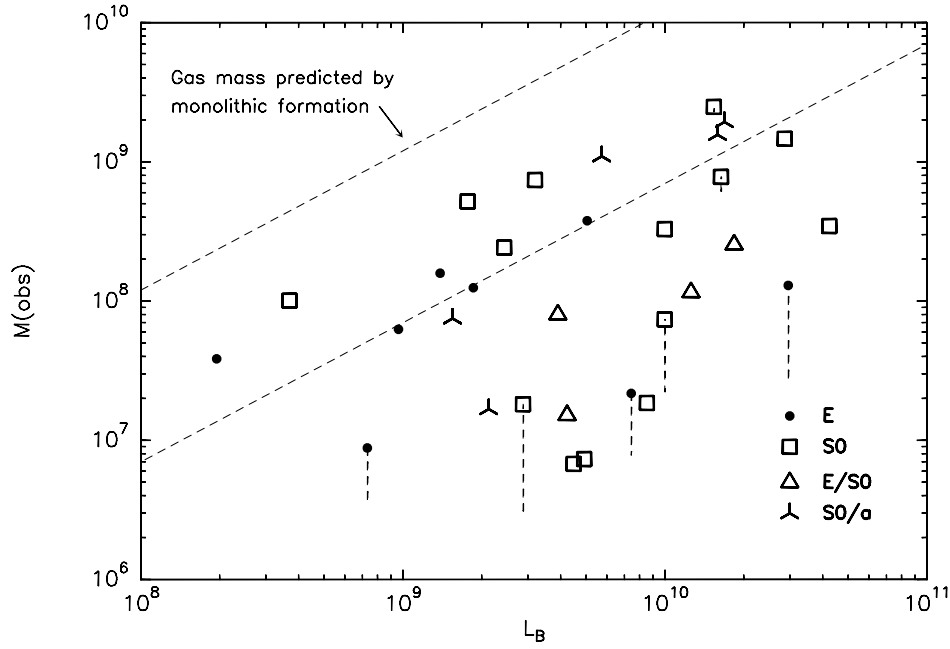


Fig. 4b.— Like Figure 4a except for galaxies in the combined E and S0 samples with the indicated classifications from the Carnegie Atlas or RC3, and which have been searched for both HI and CO and detected in at least one phase. Excluded are objects having uncertain morphological type in the above references, and confused observations as noted in the text. Dashed lines extending from data points have the same meaning as in Figure 4a.

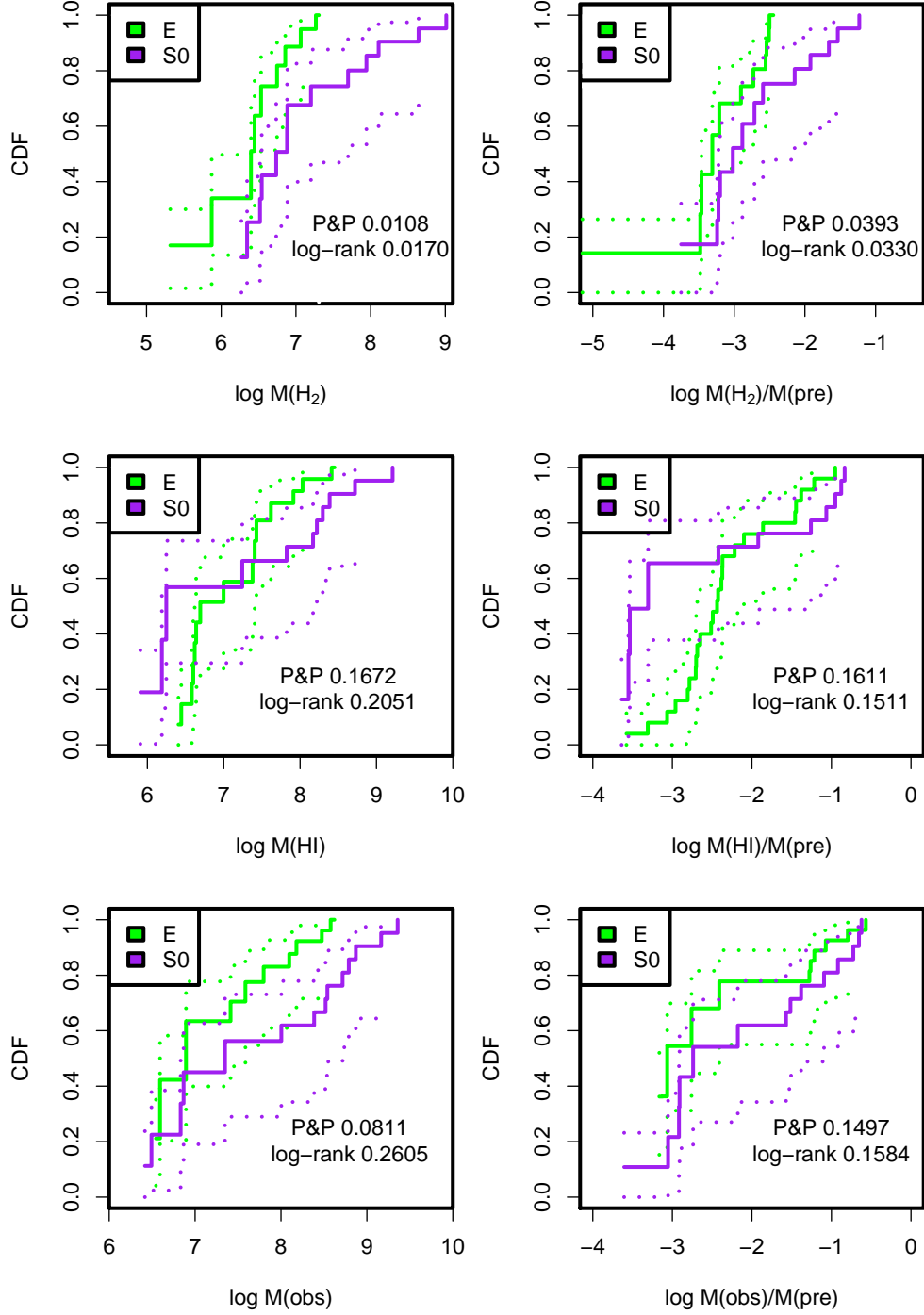


Fig. 5.— Comparisons of the Kaplan-Meier cumulative distribution functions (CDF) for the atomic, molecular, and total cool gas content of galaxies in the combined surveys, and classified E or S0 in the Carnegie Atlas or RC3. Dotted lines around each CDF trace the 95 percent pointwise confidence intervals. Insets give the probabilities that the two data sets have been drawn from the same parent population, and are derived using the log-rank and Peto-Prentice tests. Masses are in solar units.

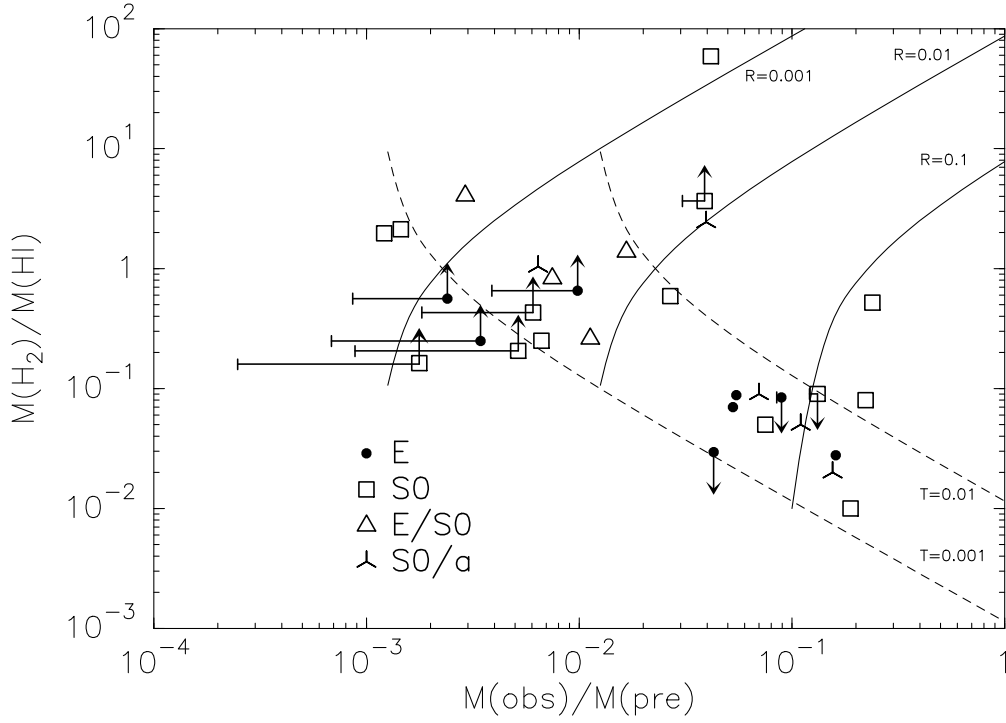


Fig. 6.— Ratio of molecular to atomic gas mass in the combined sample, for galaxies classified as explained in Figure 2. Horizontal bars connect the sum of a detection and 3-sigma limit (point) and the detection alone. Up and down arrows identify limits on $M(\text{HI})$ and $M(\text{H}_2)$, respectively. Loci of constant $R = \log[M(\text{HI})/L_B]$ and $T = \log[M(\text{H}_2)/L_B]$ are shown, respectively, by solid and dashed curves.

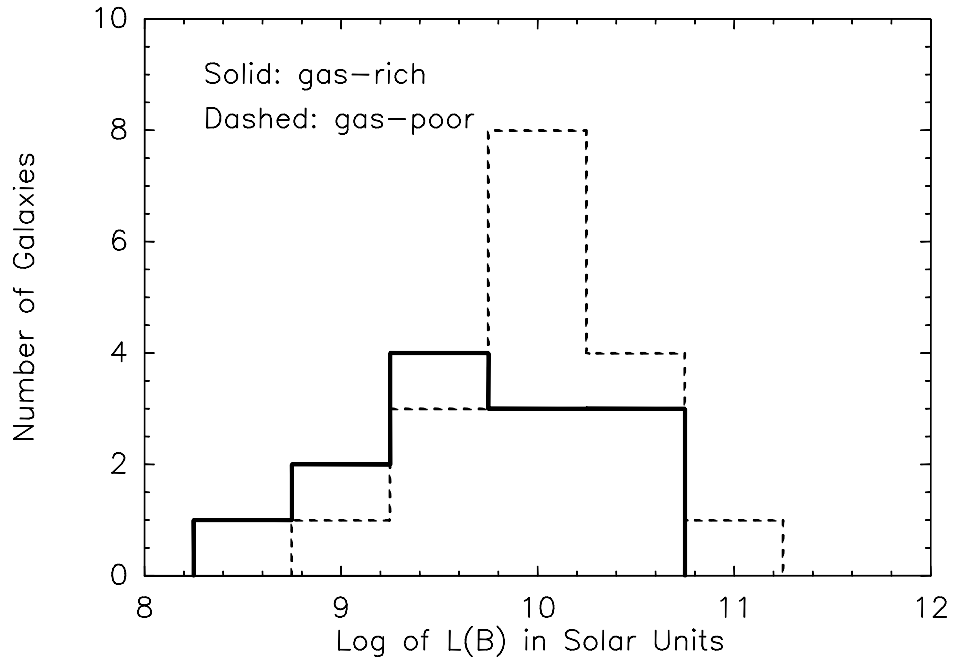


Fig. 7.— Histogram of absolute blue luminosities for galaxies in the gas-poor and gas rich clumps seen in Figure 6 and identified in Table 4.